

Research Paper

# Design and Analysis of Squeezing Ground Hydropower Tunnel in the Himalaya through a Case Study

S. Karki<sup>1</sup>, B. Karki<sup>2</sup>, B. Chhushyabaga<sup>3</sup> and S.S. Khadka<sup>4</sup>

## ARTICLE INFORMATION

### **Article history:**

### **Article history:**

Received: 14 October, 2019

Received in revised form: 10 January, 2020

Accepted: January 17, 2020

Publish on: 6 March 2020

### **Keywords:**

Assessment

Squeezing

Finite Element Analysis

Rock Mass Classification

Forepoling

## ABSTRACT

Nepal is a country with varying topography and steep fast flowing rivers, high head hydropower projects are preferred in the region. Currently, numerous hydropower tunnels are being constructed and many more have been proposed. The varying geology along with weak rock mass has created several stability problems like squeezing and support failures. Through a case study in the Lesser Himalayan Region, this paper focuses on the assessment and analysis of tunnel sections in squeezing ground through analytical and numerical modelling. The most commonly adopted Rock Mass Classification approach for estimation of tunnel support seems inadequate to address the problem associated with tunneling in the Himalayas. Therefore, the knowledge of rock mass strength and deformation behavior is required for the optimal design of tunnel support in such geological conditions. Finite element analysis is carried out for face stability of tunnel in very poor rock mass by improving the rock mass to predict the real behavior of squeezing ground. The results of the analysis show that along with the use of empirical and analytical approach, numerical analysis should be used from the preliminary stages of design and care should be taken while modelling very poor rock mass where the stability of rock ahead of tunnel face is essential.

## 1. Introduction

Nepal is a Himalayan country which covers the central part of the great Himalayan arc. The geographical distribution of the country along with the availability of large amount of water resources has created various possibilities and opportunities for the development of hydropower. More than 600 km of tunnels are currently under construction in the country. Due to the fast-flowing rivers and availability of high head, the tunnel cross section is generally small (up to 6m diameter). Majority of the tunnels are constructed in the Lesser Himalayan region of the country through drill and blast method. The method of tunnel construction by drill and blast

method disturbs the rock mass surrounding the excavation. The impact of this disturbance is greatly seen in very poor rock masses (generally in region of faults). Hence proper care must be taken during the preliminary design of the underground structures. Since the geology of the Lesser Himalaya is fragile due to tectonic activities and the presence of major folds and faults, underground excavation in the region comes along with many problems like squeezing, water inflow and even collapse of the structures. This study focuses on the use of Numerical Modelling along with analytical approach to check the stability of headrace tunnel of Sanjen Hydroelectric Project. Design of tunnel support for very poor rock mass has been done through two-dimensional

<sup>1</sup> Research Assistant and Graduate Student, Department of Civil Engineering, Kathmandu University, 44600, Dhulikhel, NEPAL, sujan.karki@ku.edu.np

<sup>2</sup> Graduate Student, Department of Civil and Environmental Engineering, Norwegian University of Science and Technology, NO-7491 Trondheim, NORWAY, bibekk@stud.ntnu.no

<sup>3</sup> Research Assistant and Graduate Student, Department of Civil Engineering, Kathmandu University, 44600, Dhulikhel, NEPAL, bimsal.chhushyabaga@ku.edu.np

<sup>4</sup> Assistant Professor, Department of Civil Engineering, Kathmandu University, Dhulikhel, 44600, NEPAL, sskhadka@ku.edu.np

Note: Discussion on this paper is open until September 2020

modelling where the face stability has been addressed by an equivalent improved rock mass around the excavation.

## 2. Case Study

### 2.1 Sanjen Hydroelectric Project (SHEP)

Sanjen Hydroelectric Project is a cascade run-of-river scheme with a capacity of 14.8 MW for Sanjen (Upper) Hydroelectric Project (SUHEP) and a capacity of 42.9MW for Sanjen Hydroelectric Project. SHEP receives the water directly from the tailrace of SUHEP and also from Chhupchung Khola and the total design discharge of SHEP is 11.57 m<sup>3</sup>/s.

The project site is located in Rasuwa District in Province 3 of Nepal, north-west of Kathmandu. With a gross head of 442m, the project has an inverted D shaped tunnel of length 3629m with dimension of 3.5x3.75 m.

#### 2.1.1 Geology

Geologically, major portion of the project lies in the Lesser Himalayan Region of Nepal with some components in the Higher Himalayan Region separated by the Main Central Thrust (MCT). Rock types of the project area are broadly classified into seven units: Garnet-Schist with Augen Gneiss, Psammitic Schist with Quartzite, White Quartzite, Graphitic Schist with Crenulated Phyllite and Slate, Psammitic Schist with Crenulated Phyllite and Quartzite, Green-grey Quartzite and Dolomitic Marble. The major rocks that dominates along the length of tunnels can be categorized into four units: Graphitic Schist, Dolomite, Quartzite and Psammitic Schist. The tunnel passes through rugged topography along the right bank of Sanjen river. The overburden varies from 34.36m to 355.33m (**Fig. 1**). The area considered for this study has a Q value ranging from 0.01 to 1.5 with moderately to wide spaced joints. Attitude of foliation is 342°/48° NE while that of joints is J1: 230°/58° and J2: 125°/76°. The orientation of major joint is oblique to the tunnel axis, dips more than 45° and drive against dip which is fair condition on excavation (Sanjen Jalavidhyut Compant Ltd., 2011).

### 2.1.2 Rock Support Estimation

**Fig. 1** shows the flow chart for estimation of support pressure. It can be seen that first step in support estimation is geological investigation which is followed by classification of rock mass according to Rock Mass Rating (RMR), Rock Mass Quality Index (Q-System) and the Geological Strength Index (GSI). If standardization of rock mass is possible then empirical approach is utilized to estimate and design the support requirement else analytical approach is followed. This result is verified after observation of face map and final tunnel support is provided.

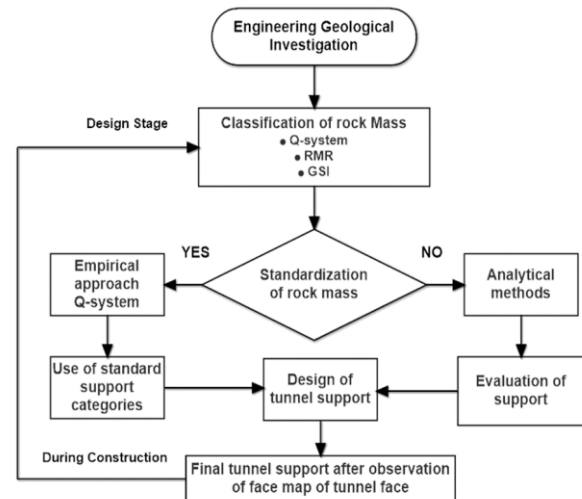


**Fig. 1.** Flow chart for tunnel support estimation (Khakda, 2019).

The Q- system of classification, proposed by Barton et al. (1974), is widely accepted classification approach. This method has been adopted on the selected case study and will be used in this study. The Q-system defines the rock quality as a function of Rock Quality Designation (RQD), Joint Set Number ( $J_n$ ), Joint Roughness Number ( $J_r$ ), Joint Alteration Number ( $J_a$ ), Joint Water Reduction factor ( $J_w$ ) and Stress Reduction Factor (SRF) and is defined as

$$Q = \frac{RQD}{J_n} * \frac{J_r}{J_a} * \frac{J_w}{SRF} \quad [1]$$

Based on the Q-value, six support class has been defined in the site and the support system provided according to it (**Table 1**).

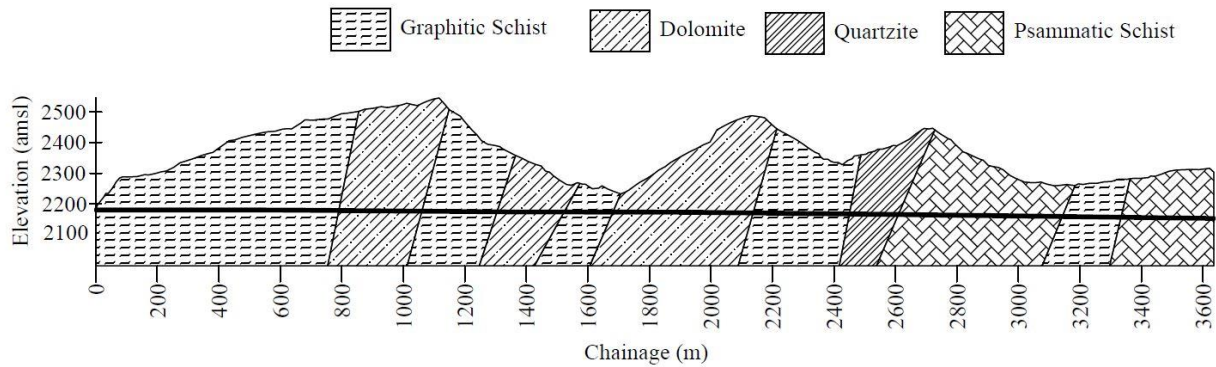


**Fig. 1.** Longitudinal Profile of geology over the Headrace Tunnel of SHEP

**Table 1.** Support class and support details provided in SHEP based on Q-value (Sanjen Jalavidhyut Compant Ltd., 2011)

Support Class	Q-Value	Support Details
S-I	>4	50 mm Fibre Reinforced Shotcrete (FRS) in mica bands, fractured area and slaking rock; spot bolting in unstable wedge and 200mm thick C20/25 grade concrete lining on invert.
S-II	1-4	50 mm thick FRS on crown, mica bands, fractured area and slaking rock; systematic bolting of 20 mm diameter rod at 1.87 m c/c spacing and 200 mm thick C20/25 grade concrete lining on invert.
S-III	0.5-1	50 mm thick FRS on crown and walls; systematic bolting of 20mm diameter rod at 1.6m c/c spacing and 200 mm thick concrete lining on invert.
S-IV	0.1-0.5	100 mm thick FRS on crown and 50mm on walls; systematic bolting of 20 mm diameter rods at 1.4 m c/c spacing and 200mm thick concrete lining on invert.
S-V	0.01-0.1	150 mm thick FRS on crown and 100 mm on walls; systematic bolting of 20 mm diameter rods at 1.2 m c/c spacing and 200mm thick concrete lining on all sides.
S-VI	<0.01	150mm thick FRS on crown and walls; systematic bolting of 20 mm diameter rods at 1 m c/c spacing; 75x150 mm steel ribs (with precast concrete lagging) at 1 m c/c spacing in seepage and falling ground; Reinforced Ribs of Shotcrete (RRS) at 1m spacing in dry area and 300mm concrete lining in all sides.

The support details provided is similar to that defined by the Q-system with an addition of concrete lining. For extremely weak section (S-VI) steel ribs are also provided which is not originally defined by the Q-system.

**2.2 Stability Assessment**

From the available sections for the selected case study, initial analysis of squeezing done according to the Singh et al. (1992) showed 13 squeezing and 22 non-squeezing sections while Jimenez and Recio (2011) showed 10 squeezing and 25 non-squeezing as shown in **Fig. 2**.

Panthi and Shrestha (2018) on their study of three hydropower tunnels in the Himalayan region developed a relation for estimating the initial and final convergence of the tunnel.

This relation (Equation 2 and 3) incorporates the stress anisotropy which is the case in almost all underground excavation. Using the relation, the convergence of the available 35 sections is found. Based on the convergence value, the sections are classified as very mild (closure <2%), mild (closure 2-3%), mild to moderate (closure 3-4%), moderate (closure 4-5%), high (closure 5-7 %) and very high squeezing (closure >7%) as defined by Singh and Goel (2011).

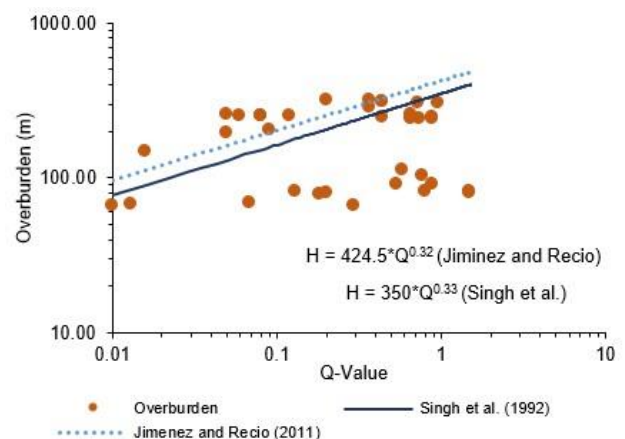


**Fig. 2.** Squeezing assessment using Singh et al. (1992) and Jimenez and Recio (2011)

The available sections were mostly dominated by Schist and among the sections, three sections suffered mild squeezing, two suffered mild to moderate squeezing while all other 30 sections had very mild squeezing (

**Table 2).**The closure values of the section have been plotted in **Fig. 3**.

$$\varepsilon_{IC} = 3065 * \left( \frac{\sigma_v * (1 + k)/2}{2G * (1 + P_i)} \right)^{2.13} \quad [2]$$

$$\varepsilon_{FC} = 4509 * \left( \frac{\sigma_v * (1 + k)/2}{2G * (1 + P_i)} \right)^{2.09} \quad [3]$$

Where  $\varepsilon_{IC}$  and  $\varepsilon_{FC}$  represent instantaneous and final closure in mm,  $P_i$  is the support pressure in MPa,  $G$  is the shear modulus and  $\sigma_v$  is the vertical pressure both in MPa and  $k$  is the in-situ stress ratio.

Other parameters are calculated according to the relations defined later in Section 4.1.

From the available sections three different sections have been selected, each representing a different rock class. Sections at chainage 1+759.88, 2+137.7 and 2+240.3 representing poor, very poor and extremely poor rock class (S-II, S-III and S-V) with varying overburden have selected for numerical modelling. **Table 1** provides the support details for the selected sections. The sections at Ch. 1759.88 and 2137.70 m suffer very mild squeezing while section at Ch. 2240.30 m suffer mild to moderate squeezing according to the classification done by Singh and Goel (2011)

**Table 2.** Calculation of Closure for tunnel sections of Sanjen HEP

Chainage (m)	Q-value	H (m)	$\sigma_v$ (MPa)	$\sigma_h$ (MPa)	$P_i$ (MPa)	G (MPa)	Closure (mm)	
							$\varepsilon_{IC}$	$\varepsilon_{FC}$
1+563.23	0.54	91.25	2.46	4.36	0.146	1158.61	2.39	4.58
1+565.10	0.89	90.00	2.43	4.33	0.161	1402.82	1.60	3.08
1+584.72	0.81	82.20	2.22	4.26	0.155	1353.14	1.57	3.03
1+587.73	0.13	81.00	2.19	4.32	0.146	671.81	4.90	9.26
1+590.86	0.2	79.75	2.15	4.29	0.184	792.21	3.59	6.83
1+596.00	0.181	77.71	2.10	4.27	0.282	762.52	3.75	7.13
1+635.30	0.069	68.14	1.84	4.21	0.322	527.20	6.34	11.92
1+637.95	0.013	67.55	1.82	4.26	0.322	278.38	17.40	32.12
1+643.08	0.01	66.38	1.79	4.26	0.354	251.79	19.84	36.53
1+645.49	0.293	66.56	1.80	4.15	0.376	1313.37	1.08	2.10
1+756.88	1.5	79.56	2.15	4.21	0.161	2453.92	0.42	0.83
1+759.88	1.5	81.42	2.20	4.23	0.194	2453.92	0.43	0.85
1+794.65	0.778	103.03	2.78	4.45	0.194	1908.61	0.91	1.77
1+808.77	0.58	111.81	3.02	4.55	0.156	1705.67	1.12	2.18
1+864.11	0.016	146.23	3.95	5.14	0.142	431.72	16.90	31.22
1+938.46	0.05	192.45	5.20	5.54	0.184	667.62	12.25	22.75
1+957.55	0.09	204.32	5.52	5.60	0.184	836.00	9.08	16.97
2+094.60	0.2	316.58	8.55	6.63	0.238	1134.79	10.37	19.32
2+117.00	0.44	311.78	8.42	6.47	0.310	1534.52	5.75	10.84
2+118.20	0.44	311.12	8.40	6.46	0.376	1534.52	5.73	10.81
2+135.30	0.96	301.72	8.15	6.26	0.548	1569.41	5.52	10.41
2+137.70	0.72	300.40	8.11	6.29	0.168	1405.76	6.79	12.76
2+160.70	0.37	315.00	8.51	6.52	0.101	1089.54	11.95	22.20
2+164.50	0.37	285.67	7.71	6.24	0.082	1089.54	10.20	19.02
2+234.10	0.66	257.50	6.95	5.90	0.082	1359.71	5.68	10.70
2+240.30	0.05	257.50	6.95	6.23	0.210	506.53	34.14	62.22
2+242.70	0.06	250.00	6.75	6.12	0.640	543.13	28.97	52.96
2+244.30	0.08	250.00	6.75	6.09	0.587	606.33	23.97	43.97
2+245.60	0.08	250.00	6.75	6.09	0.338	606.33	23.97	43.97
2+248.40	0.12	250.00	6.75	6.04	0.246	708.10	18.24	33.64
2+251.30	0.44	247.50	6.68	5.85	0.238	1164.25	7.19	13.49
2+256.70	0.88	247.50	6.68	5.77	0.274	1518.00	4.31	8.17
2+259.10	0.74	242.50	6.55	5.75	0.075	1420.58	4.76	9.00
2+263.80	0.66	240.00	6.48	5.74	0.073	1359.71	5.10	9.63
2+266.00	0.88	240.00	6.48	5.70	0.086	1518.00	4.12	7.81

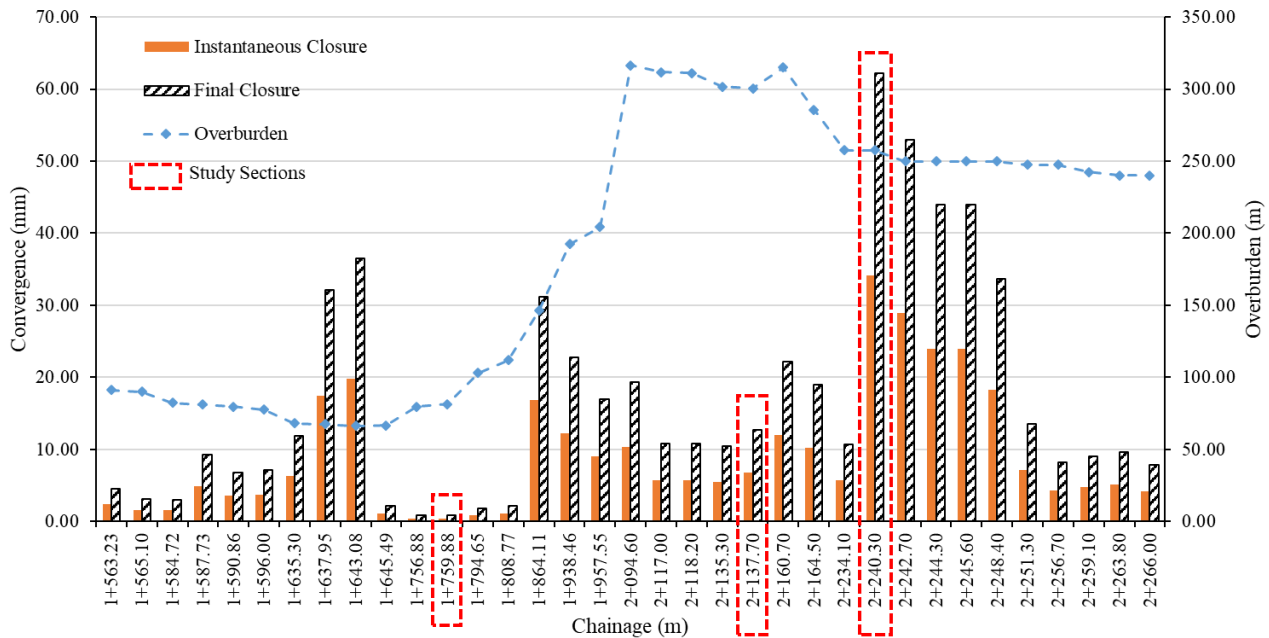


Fig. 3. Comparison of Tunnel closure for tunnel sections

### 3. Rock Support Interaction – Characteristic Curve

The Convergence Confinement method (CCM) of rock support interaction suggested by Carranza-Torres and Fairhurst (2000) is one of the popular methods of analytic approach for support design. This method assumes a circular tunnel of radius  $R$  subjected to a uniform isotropic field stress  $\sigma_0$ . Carranza-Torres and Fairhurst (2000) have explained the effect of tunnel face for the stability of section as the support does not carry the full load of the earth pressure where it is installed. Some part of the load is carried by the tunnel face and as the face moves farther from the section under consideration, the load on the support increases. When a tunnel face is about twice the tunnel diameter far from the section considered, only then the maximum deformation occurs in the section. Similarly, the deformation is zero not on the face of the tunnel but about twice diameter of tunnel ahead of the face. This is represented by a curve known as the Longitudinal Deformation Profile (LDP). Ground Reaction Curve (GRC) and Support Characteristic Curve (SCC) are the other two curves of CCM. GRC shows the nature of the ground as the tunnel is excavated. Initially the ground is in elastic state and as the tunnel is excavated, its nature changes to plastic. The SCC on the other hand defines the capacity of the support installed in the section. The interaction of the GRC and the SCC gives the amount of pressure that the support must bear and the deformation that occurs during the installation and after the support has taken the full load imposed over it. The plot of GRC and SCC for the selected sections (Ch. 1759.88, 2137.70 and 2240.30 m) is shown in Fig. 4.

The LDP is used to relate the deformation perpendicular to the tunnel axis with the position along the axial direction

(i.e. it is used to predict the amount of radial deformation at various position along the axis of the tunnel). Due to this reason, the LDP is very much essential as it is used to determine the location for installation of support. Vlachopoulos and Diederichs (2009) proposed an improved version of LDP by relating it to the normalized plastic radius of the tunnel (plastic radius/tunnel radius). Since the development of plastic zone around the tunnel affects its stability, it becomes very important to identify the location for support installation. Delayed installation can lead to failure of the tunnel while early installation demands stiffer and heavy support which can unnecessarily increase the cost of the project.

The improved LDP requires maximum wall displacement and maximum plastic radius as input which can be obtained by a simple plane strain analysis or by the relation proposed by Carranza-Torres and Fairhurst (2000). For this study, this improved version of LDP (Fig. 5) will be used where the maximum plastic radius and deformation is obtained from Carranza-Torres and Fairhurst (2000). The support is then provided which is used to find the pressure the support system must bear and in turn the final convergence after the support takes the full load imposed on it (Fig. 4).

The LDP proposed by Vlachopoulos and Diederichs (2009) is also for a circular tunnel under isotropic stress state. Since the tunnel of study is inverted D shaped under anisotropic stress, Vlachopoulos and Diederichs (2014) studied the use of the LDP in non-circular excavation in anisotropic stress state. According to their study, this LDP proposed for circular excavation can be well used for non-circular case too provided the aspect ratio of the tunnel is small. Similarly, for anisotropic condition, the authors, on their preliminary analysis state that the LDP based on  $K=1$  can be used to calibrate the 2D models using the direction of maximum yield i.e. the direction of minimum stress. The LDP,

in this study has been prepared considering the given conditions.

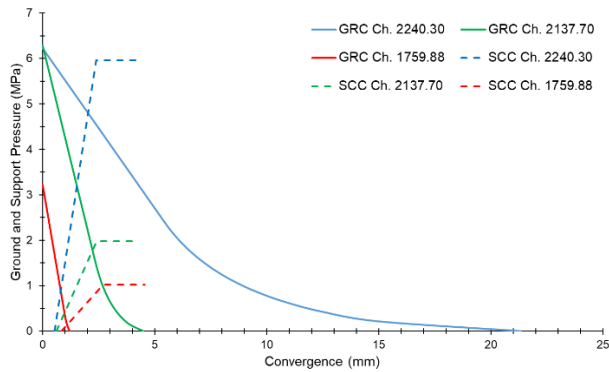


**Fig. 4.** Plot of Ground Reaction Curve and Support Characteristic Curve for the selected sections

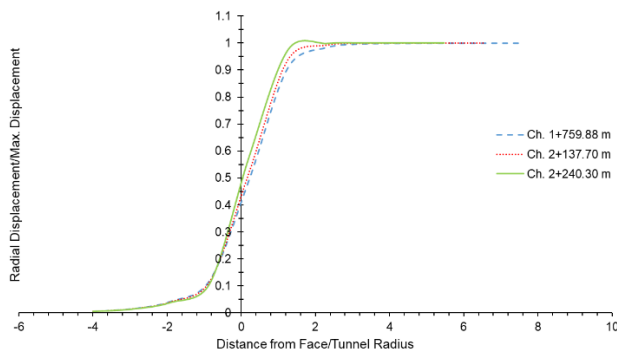


**Fig. 5.** Longitudinal Deformation Profile for selected section according to the relation proposed by Vlachopoulos and Diederichs (2009)

#### 4. Numerical Modelling

Underground excavation is practically a three-dimensional problem (Vlachopoulos & Diederichs, 2014). The behavior of ground during the excavation process can be represented accurately by a 3D modelling technique, but the time and complexity of using such techniques makes it difficult to be used for analysis of every section along the excavation. Due to this, two-dimensional modelling software is widely used for the analysis and design of underground structures. Many researches have been done to simulate the 3D effect of tunneling through 2D approach. Vlachopoulos and Diederichs (2014) state that in order to accurately simulate the loading of the support or the effects of sequential excavation, the 2D model must capture the pre-face conditions, the state of displacement and plasticity at the face and the subsequent development of deformation and yielding. By creating a staged model where an internal pressure is applied to represent the in-situ condition (before tunnel excavation) and by gradually reducing the internal pressure over a number of stages until the internal pressure is zero (this represents the excavated condition), the effects of 3D excavation can be studied by 2D analysis. As the internal pressure is reduced, the rockmass surrounding the

excavation yields and a plastic zone develops around the tunnel. This gradual reduction of internal pressure also leads to increasing deformation within the model.

Among the various software available for modelling of underground excavation, one of the popular software based on finite element modelling technique, Phase<sup>2</sup>, has been used in this paper. Phase<sup>2</sup> developed by RocScience is a 2D, finite element method-based software that can model ground behavior by elastic-plastic, strain softening/hardening method. It allows to model an underground excavation efficiently where the rock behaves as plastic around the excavation and behaves as elastic far from the excavation (Khadka et al., 2019).

Among the various failure pattern of rock, the Hoek Brown criteria was developed by studying the brittle failure of intact rock and jointed rock mass. Hoek and Brown developed the criteria for intact rock and introduced factors to reduce its properties based on joints in rock mass (Hoek, Torres, & Corkum, 2002). Later this criterion was modified to incorporate variable rock mass and was introduced as Generalized Hoek Brown failure criteria.

##### 4.1 Estimation of rock parameters

In this study the rock mass has been modelled from Generalized Hoek Brown failure criteria. This empirical failure criterion establishes the strength of rock mass in terms of major and minor principle stresses and is expressed as follows:

$$\sigma_1 = \sigma_3 + \sigma_{ci} \left( m_b \frac{\sigma_3}{\sigma_{ci}} + s \right)^a \quad [4]$$

$\sigma_1$  and  $\sigma_3$  are the major and minor principle stress,  $\sigma_{ci}$  is the uniaxial compressive strength of intact rock,  $m_b$ ,  $s$  and  $a$  are the rock constants which depend upon the characteristics of the rock mass (Hoek, Torres, & Corkum, 2002).

This criterion predicts strengths that agree well with values determined from laboratory triaxial tests of intact rocks, and from observed failures in jointed rock masses (RocScience, 2019). Since it is not always possible to obtain the laboratory values through triaxial test on the rock mass, Hoek and Brown provided a means to estimate the materials constants  $m_b$ ,  $s$  and  $a$  through empirical relation, which can be found in the original paper.

Other parameters required for the application of the failure criterion in Phase<sup>2</sup> is the Geological Strength Index (GSI) and Rock mass modulus ( $E_{rm}$ ). GSI is obtained by the relation provided by Hoek and Diederichs (2006) (Equation 5). RMR here refers to the equivalent Rock Mass Rating value obtained from the Q-value as given by Equation 6 (Barton, 1995). Rock mass modulus is obtained from the equation suggested by Hoek and Brown (Hoek, Torres, & Corkum, 2002) and is given in Equation 7

$$GSI = RMR - 5 \quad [5]$$

$$RMR = 15 * \log(Q) + 50 \quad [6]$$

$$E_{rm}(GPa) = \left(1 - \frac{D}{2}\right) \sqrt{\frac{\sigma_{ci}}{100}} * 10^{\left(\frac{GSI-10}{40}\right)} \quad [7]$$

Where the term D refers to the disturbance factor which ranges from 0 (undisturbed rock) to 1 (very disturbed rock) (Hoek, Torres, & Corkum, 2002).

For vertical stress ( $\sigma_v$ ) and horizontal stress ( $\sigma_h$ ), the relations 8 and 9 has been used (Panthi & Shrestha, 2018).

$$\sigma_v = \gamma * H \quad [8]$$

$$\sigma_h = \frac{\nu}{1-\nu} \sigma_v + \sigma_{tech} \quad [9]$$

Here the parameters  $\gamma$  refers to unit weight of rock mass which is taken as 0.027 MN/m<sup>3</sup>(Carranza-Torres & Fairhurst, 2000), H is the overburden in meters,  $\nu$  is the poisons ratio of the rock, taken as 0.2 which agrees with the value given by Gercek (2006) for the rock class and that obtained from the relation given by Hoek et al. (1995) and  $\sigma_{tech}$  is the tectonic stress. Since the headrace tunnel is aligned to North South direction as that of the tectonic stress, the tectonic component of stress was taken as 3.5 MPa for the site (Panthi & Shrestha, 2018). Due to the addition of tectonic stress, in instances where the vertical stress is less than tectonic stress, the horizontal stress value exceeds the vertical stress value as in the case of Chainage 1759.88 m. All other obtained values are given in **Table 3**. During modelling of the sections, the disturbance factor (D) has been taken as 0.5 and the rock constant ( $m_i$ ) has been taken as 11.

**Table 3.** Rock mass properties of selected sections for Numerical Modelling

Chainage (m)	H (m)	GSI	$\sigma_{ci}$ (MPa)	$E_{rm}$ (MPa)	$\sigma_v$ (MPa)	$\sigma_h$ (MPa)
1759.88	81.42	48	136.84	6.127	2.20	4.23
2137.70	300.40	43	78.77	3.530	8.11	6.29
2240.30	257.50	25	78.77	1.298	6.95	6.23

#### 4.2 Rock modelling

Methodologies commonly employed to represent the 3D effects of tunneling by 2 D modelling are by straight excavation, average pressure reduction, excavation of concentric rings and face de-stressing (with or without softening) (Vlachopoulos & Diederichs, 2014). In this paper, the face replacement technique with material softening (reduction of modulus of the surrounding materials) has been used. In face replacement, the tunnel core is replaced with an unstressed, elastic material in each stage and the tunnel boundary is allowed to converged until a temporary equilibrium is reached This face replacement can be made more efficient by softening of each core replacement which results in an efficient excavation sequence (Vlachopoulos &

Diederichs, 2014). Details on other techniques can be found in the original paper and will not be explained here.

The reduction of modulus technique used in this paper is a representation of reducing face effect during a tunnel excavation. By knowing the amount of deformation prior to support installation, the modulus value which yields the obtained deformation can be found and the support can be installed in that particular stage. Anisotropic stress condition is taken and the rock mass is modelled as strain-softening and elastic-plastic model, based on the GSI value. For estimating the residual values for application of strain softening model, Cai et al. (2007) performed analysis by reducing the block volume and joint condition factor and the obtained residual values were found consistent with the in-situ test data. Similarly, through numerical analysis of eight different case studies from the Himalayan Region, Khadka (2019) suggested using a residual value of 50 to 60% of peak GSI for fair to good rocks (50<GSI<65), 30 to 40% of peak GSI for very poor to poor rocks (30<GSI<50) and peak GSI (i.e. no reduction in peak GSI) for extremely weak rock (GSI<30). This result of modelling was in well agreement with the results of Cai et al. (2007). Since SHEP also lied in the Himalayan Region, the results of Khadka (2019) will be referred in this study. However, the mechanical properties ( $\sigma_{ci}$  and  $m_i$ ) have not been changed as suggested by Cai et al. (2007).

In the study, horizontal stress is taken as the major principle stress and vertical as minor. Whenever the vertical stress exceeds the horizontal, the stress is rotated by 90 degrees to represent the insitu condition. Tunnel support was provided according to that defined in the actual site and its stability was checked against the imposed stress. The input parameters for modelling are provide in **Table 3** and the properties of the support are provided in **Table 4**.

**Table 4.** Material Properties of Supports

Parameters	Unit	Shotcrete	Concrete	Steel Rib
Young's Modulus	GPa	30	34	200
Poisson's Ratio		0.25	0.2	0.25
Cross sectional area	mm <sup>2</sup>			2810
Moment of Inertia	mm <sup>4</sup>			1.51x10 <sup>7</sup>
Section depth	mm			175

#### 4.3 Results of Numerical Analysis

On analysis of the selected sections of the tunnel, it was seen that the support provided in the site was not sufficient except in section at Ch. 1759.88 m with poor rock mass. In the section, numerical modelling showed that the provided support (**Table 1**) was safe except on the corners, where the stress accumulation is maximum. In order to address the problem at the corners of invert, additional support must be provided as suggested by Khadka et al. (2019). It was seen that a total of 600mm concrete of 45 MPa strength was required to withstand the stress. Since providing such a huge amount of support increases the cost of the project, if the

excavation can be done making a curvature profile at the corners, the support requirement can be greatly reduced. As in the case of sharp corners, the stress acting in two different direction (vertical and horizontal) gets concentrated at a single point which is avoided in the curve profile. Due to the curve profile, the incoming stress tends to redistribute around the curvature by decrease in radial stress and increase in tangential stress. As a result, stress concentration at a single point is reduced and gets uniformly distributed around the profile due to which fewer support are sufficient to withstand the imposed stress. It was seen that on round corners as shown in **Fig. 6** (b), the amount of support to withstand the imposed stress is reduced to 50 mm of shotcrete. The support capacity plot for sharp corners and round corners of invert is provided in **Fig. 7**. As can be seen in the figure, some of the points lie outside the curve for sharp corners meaning the provided support is insufficient which results in failure of the support in moment which is not the case for round corners as all the points lie well inside the factor of safety curve.

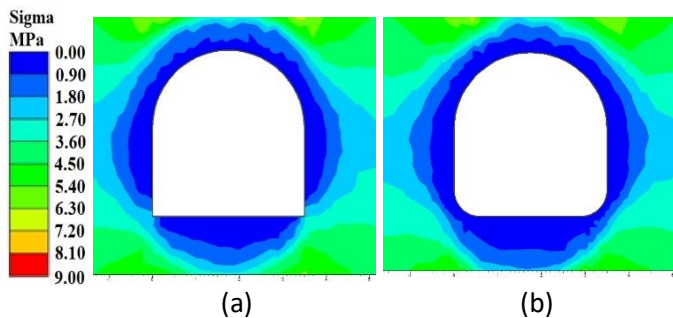


**Fig. 6.** Mean Stress Distribution around the tunnel excavation (a) with sharp invert corners and (b) with round invert corners. Redistribution of stresses takes place in the round corners resulting in low support requirement compared to the sharp invert corners.

Similarly, for section at Ch. 2137.70m, the support criteria defined in the site was insufficient. The section had a Q-value of 0.72 which required the support according to class III (**Table 1**) but on modelling the section with the given support, failure of the tunnel walls was seen. Increasing the shotcrete thickness to 100mm proved to be safe for the section. However, the thickness of the invert showed a failure at the corners as in previous section (Ch. 1759.88m). Providing a curvature profile to the corners, as presented earlier will avoid increasing the thickness of the invert lining while safely withstanding the stress.

In the other section (Ch. 2240.30), the support was not enough to withstand the high stress. With the large overburden and extremely poor rock class, the support requirement is very high. The support defined by the Q-system and that provided in the site seems insufficient (**Fig. 8**). Providing steel ribs in addition to the defined support also was not sufficient to address the weak rocks. For such weak rocks, face stability must be done in addition to providing support. Providing temporary support to the face helps to stabilize the face in addition to providing a safe working environment to the workers and also provides some degree

of stability to the adjacent sections. The behavior of the earth material (core) ahead of the tunnel face affects the process of tunneling in squeezing ground (Hoek, 2001). Thus, it is important to understand its nature and take preventive measures for successful tunneling.

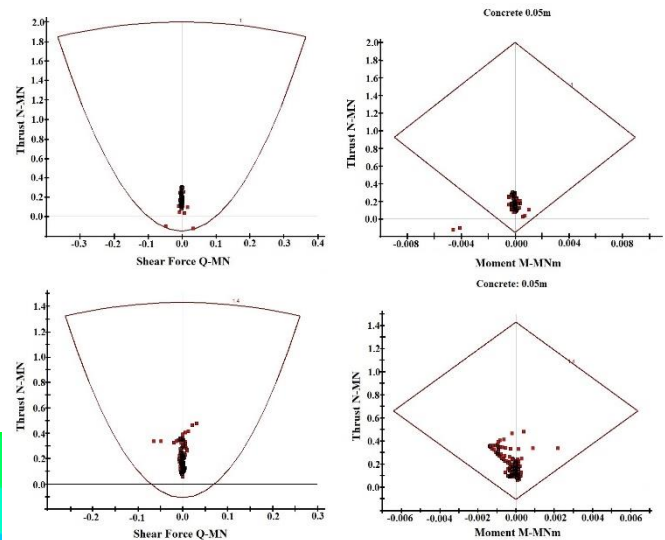


**Fig. 7.** Support Capacity Plot of 50mm SRF for sharp invert corners (top) with Factor of Safety 1 and Round invert corners (bottom) with Factor of Safety 1.4

#### 4.3.1 Tunneling in squeezing ground

While tunneling through squeezing ground, the stability of the rock mass surrounding the excavation can be achieved by grouted pipe forepoling, grout injection or by reinforcement with grouted fiberglass dowels (Hoek, 2001). To achieve the reinforcement of rock mass ahead of the tunnel face, complete 3D analysis is required where the forepoles are installed as a structural element to reinforce the rock mass (Hoek, 2001). This procedure, however cannot be achieved through a 2D analysis, where the rock mass surrounding only the particular section under consideration can be studied. The axisymmetric approach available in RS2 can be used to investigate simple three-dimensional problems but it does not give all the detailed behavior of the tunnel section under consideration.

In order to simulate the effect of grouted pipe forepole in a two-dimensional plane strain analysis, a zone of improved rock is provided around the arch of the excavation as suggested by Hoek (2001). By taking the weighted average of strength and deformation properties of the rock, forepole pipe and grout material, an improved rock mass equivalent to the obtained strength is provided around the excavation. Hoek (2001) says that this estimate of improved rock mass confirms with the actual tunnel performance constructed with forepole umbrellas. During the modelling, a forepole pipe with 114 mm external diameter and 100 mm internal diameter and 12 m long installed every 8 m to obtain an overlap of 4 m is used. The forepole is assumed to be spaced 500 mm apart centre to centre and the strength of grout is taken as 30MPa.

This gives a strength of 2.5MPa and other parameters required for the rock mass were obtained from Hoek (2004).

**Table 5.** Parameters for improved rock mass

Parameters	Value
Geological Strength Index (GSI)	25
Hoek Brown Constant ( $m_i$ ):	8
Intact Rock strength ( $\sigma_{ci}$ ):	29.5 MPa
Rock mass strength ( $\sigma_{cm}$ ):	2.5 MPa
Deformation modulus (E):	1288 MPa
Hoek Brown Constant ( $m_b$ ):	0.549
Hoek Brown Constant (s):	0.0002
Hoek Brown Constant (a):	0.531

The forepole is provided during the softening of the rock mass (i.e. when the modulus is reduced by 50%). From the analysis of previous sections (Ch. 1759.88 and 2137.70m) and from the results from Khadka et al. (2019), the sections at Ch. 2240.3 m is modified to obtain a curvature at the corners of invert, in order to limit the amount of lining at the location.

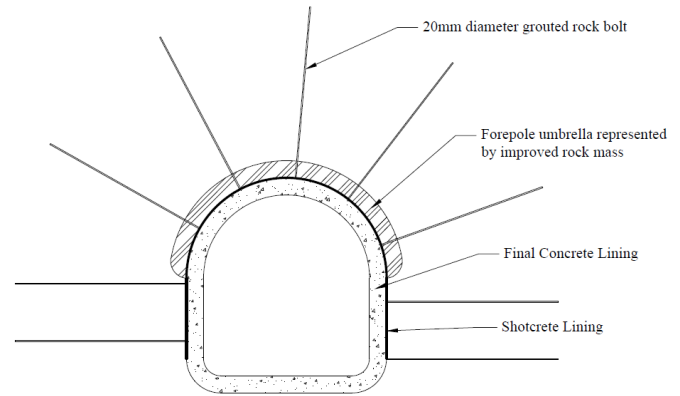


**Fig. 9.** Support to extremely poor rock mass at Ch. 2240.3m

**Table 6.** Results from Numerical Analysis for extremely poor section

Displacement (mm)		Remarks
Crown	Invert	
35.6	42	Unsupported
16	23	Observed support
<b>For modified support</b>		
5.9	6.4	Installation of forepole umbrella
11.4	17.4	Installation of rock bolt
11.3	18.2	Installation of liners

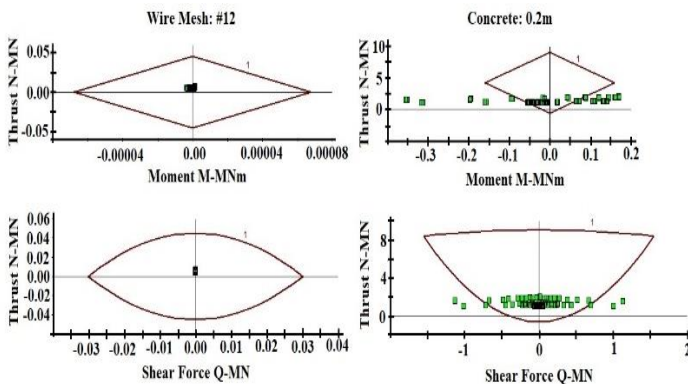


**Fig. 8.** Support Capacity Plot for Observed support at Ch. 2240.3 m

After the application of forepole umbrella, a support of 100mm shotcrete lining with 157mm depth steel section embedded in 200mm of concrete lining was provided with resulted in safe support to the excavation. Grouted rock bolt of 3m length, 20mm diameter at 1m c/c spacing was also provided initially to strengthen the rock mass (Fig. 9). The deformation at the crown and wall at various stages have been provided in Table 6.

From the table it can be seen that the convergence has been reduced by a great amount and the results of numerical analysis also showed safety of support against failure. Note that the forepole is installed after the softening of the rock mass so some amount of deformation has already occurred during its installation. In the invert, however, the concrete lining thickness has been increased to 700mm along with invert struts. An option to limit the thickness in the invert would be delayed support installation which allows the invert to further deform and at a later time, the converged section can be excavated prior to the lining.

This practice of delayed installation of invert support is also common during tunneling in the Himalayas and help reduce the amount of support requirement in the invert. Although some footing must be provided in the corners of the invert to prevent the failure of the wall support in such a squeezing section.

On comparison of convergence obtained from empirical (Panthi & Shrestha, 2018), Convergence Confinement Method (Carranza-Torres & Fairhurst, 2000), (Vlachopoulos & Diederichs, 2009) and Numerical Modelling, it was seen that deformation obtained from modelling was greater than that obtained from the other two methods (Fig. 10). Although improvements have been made to consider anisotropic condition in empirical and non-circular excavation in analytical solution (Vlachopoulos & Diederichs, 2014), the disturbance of the surrounding rock mass during construction has not been considered. This disturbance has a great impact on the stability of excavation as a result of which the obtained convergence was greater in numerical modelling. This effect can be clearly seen for weak rock with high overburden (Chainage 2137.7 m). The disturbance factor assigned during modelling accounts for the damage to the surrounding rockmass during excavation and for weak rocks, the damage is severe. Such damaged rocks tend to deform more and if left unchecked can result collapse. Due to this, the convergence obtained from numerical modelling is very high compared to the analytical and empirical approach for the given chainage. Some discrepancies might be present as all

the parameters for modelling were not obtained from the in-situ tests so assumptions were made which might differ from the actual site condition.

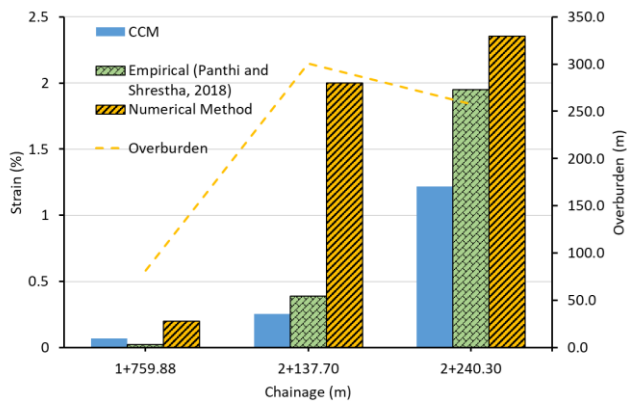


**Fig. 10.** Comparison of strain from empirical, analytical and numerical solutions for selected sections

## 5. Conclusions

In this paper, the support system provided in headrace tunnel of Sanjen Hydroelectric project was studied using analytical and numerical method. From the study it was concluded that analytical method, CCM, is not sufficient for very weak rock mass as it underestimates the final convergence value as seen from the GRCs in **Fig. 4**. CCM demands support in the early stage of excavation resulting in heavy support requirement. However, providing support at such earlier time is not economical as some amount of deformation must be allowed before support installment.

Similarly, for numerical modelling, special care must be taken while modelling squeezing ground by 2D modelling. For very poor rock mass, the behavior of rock mass ahead of tunnel must also be studied along with that surrounding the excavation. During excavation in extremely weak sections, forepoling is done to strengthen the rock mass ahead of the tunnel face. By improving the rock mass surrounding the boundary of excavation, umbrella forepole can be simulated in 2D modelling. From this study, it is clear that only empirical design method is not sufficient to stabilize the excavation. Numerical modelling by simulating forepole umbrella can help achieve safe and economical support systems. Thus, numerical modelling must be carefully implemented from the designing phase of project and special attention must be paid to the very weak rock masses and the modelling done with great care for safety of the project and workers. Since no proper measurement of deformation was made in the selected project, the results of numerical modelling cannot be quantitatively validated. Instead, this study aims in studying the methodology of numerical modelling for squeezing ground, given by Terzaghi, with reference to Himalayan geology and the results are in good agreement with the practical scenario.

## Acknowledgements

The authors would like to express their sincere gratitude for financial supports from the University Grant Commission and Faculty Research Grant under grant UGC/FRG-73/74-ENGG-03.

## References

- Barton, N., 1995. The influence of joint properties in modelling jointed rock masses. 8th ISRM Congress. Keynote lecture, Tokyo: 1023-1032.
- Barton, N., Lien, R., & Lunde, J., 1974. Engineering classification of rock masses for the design of tunnel support. *Rock Mechanics*, **6** (4): 189-239.
- Cai, M., Kaiser, P., Tasaka, Y., & Minami, M., 2007. Determination of residual strength parameters of jointed rock masses using the GSI system. *International Journal of Rock Mechanics & Mining Sciences*, **44**: 247-265.
- Carranza-Torres, C., & Fairhurst, C., 2000. Application of convergence confinement method of tunnel design to rock masses that satisfy the Hoek Brown failure criteria. *Tunnelling and underground space technology*, **15**: 187-213.
- Gercek, H., 2006. Poisson's ratio values for rocks. *International Journal of Rock Mechanics & Mining Sciences*, **44**: 1-13.
- Hoek, E., 2001. Big Tunnels in Bad Rocks-2000 Terzaghi Lecture. *ASCE Journal of Geotechnical and Geoenvironmental Engineering*, **127** (9): 726-740.
- Hoek, E. (2004). Numerical Modelling for Shallow Tunnels in WeakRock. Retrieved from rocsience: <https://www.rocsience.com/assets/resources/learning/papers/Numerical-Modelling-for-Shallow-Tunnels-in-Weak-Rock.pdf>
- Hoek, E., & Diederichs, M., 2006. Empirical Estimation of Rock Mass Modulus. *Int. Journal of Rock Mech. & Mining Sciences*, **43**: 203-215.
- Hoek, E., Kaiser, P., & Bawden, W., 1995. Support of Underground Excavation in Hard Rock. CRC Press.
- Hoek, E., Torres, C. C., & Corkum, B., 2002. Hoek-Brown Failure Criteria - 2002 edition. Proceedings North American rock mechanics society meeting. Toronto.
- Jimenez, R., & Recio, D., 2011. A linear classifier for probabilistic prediction of squeezing conditions in Himalayan tunnels. *Engineering Geology*, **121**: 101-109.
- Khakda, S. (2019). Tunnel Closure Analysis of Hydropower Tunnels in Lesser Himalayan Region of Nepal through Case Studies. Retrieved from Rock Mechanics and Underground Structure Lab: [http://rmlab.ku.edu.np/wp-content/uploads/2019/09/PhD-Thesis\\_\\_Fulltext\\_\\_Fulltext.pdf](http://rmlab.ku.edu.np/wp-content/uploads/2019/09/PhD-Thesis__Fulltext__Fulltext.pdf)
- Khakda, S., Karki, S., Chhushyabaga, B., & Maskey, R., 2019. Assessment and Numerical Analysis of Hydropower Tunnels in Lesser Himalayan Region of Nepal-A Case Study. *Journal of Physics: Conf. Series* **1266**.
- Panthi, K., & Shrestha, P., 2018. Estimating Tunnel Strain in the Weak and Schistose Rock Mass Influenced by Stress Anisotropy: An Evaluation Based on Three Tunnel Cases from Nepal. *Rock Mechanics and Rock Engineering*, **51** (6): 1823-1838.
- RocScience. (2019). Generalized Hoek Brown Criterion. Retrieved from rocsience:

- [https://www.rocsience.com/help/rocdata/rocdata/Generalized\\_Hoek-Brown\\_Criterion.htm](https://www.rocsience.com/help/rocdata/rocdata/Generalized_Hoek-Brown_Criterion.htm)  
 Sanjen Jalavidhyut Compant Ltd., 2011. Feasibility Study Report Volume I: Main Report. Kathmandu: Sanjen Jalavidhyut Compant Ltd.  
 Singh, B., & Goel, R., 2011. Engineering Rock Mass Classification. India: Butterworth Heinemann Publication.  
 Singh, B., Jethwa, J., Dube, A., & Singh, B., 1992. Correlation between observed support pressure and Rock Mass Quality. Tunnelling and Underground Space Technology 7(1), 59-74.  
 Vlachopoulos, N., & Diederichs, M., 2009. Improved Longitudinal Displacement Profiles for Convergence Confinement Analysis of Deep Tunnels. Rock Engineering and Rock Mechanics 42: 131-146.  
 Vlachopoulos, N., & Diederichs, M., 2014. Appropriate Uses and Practical Limitations of 2D Numerical Analysis of Tunnels and Tunnel Support Response. Geotechnical and Geological Engineering, 32 (2): 469-488.

$\sigma_{tech}$	Tectonic component of stress
K	Stress Ratio
$m_i$	Material constant for intact rock
$m_b, s, a$	Hoek Brown Constants
$P_i$	Support Pressure
G	Shear Modulus
$\epsilon_{iC}$	Instantaneous Closure
$\epsilon_{iC}$	Final Closure
GSI	Geological Strength Index
$\gamma$	Unit Weight of rock
$\nu$	Poisson's Ratio
$E_m$	Young's Modulus of Rock Mass
Q	Rock Quality Index
RQD	Rock Quality Designation
$J_n$	Joint Set Number
$J_r$	Joint Roughness Number
$J_w$	Joint Water Reduction Factor
SRF	Stress Reduction Factor
FRS	Fibre Reinforced Shotcrete
CCM	Convergence Confinement method
LDP	Longitudinal Displacement Profile
GRC	Ground Reaction Curve
SCC	Support Characteristic Curve
GSI	Geological Strength Index
RMR	Rock Mass Rating
D	Disturbance Factor

### Symbols and abbreviations

H	Overburden
$\sigma_v$	Vertical Pressure
$\sigma_h$	Horizontal Pressure
$\sigma_{ci}$	Intact Rock Strength
$\sigma_{cm}$	Rock Mass Strength
$\sigma_o$	In-situ field stress
$\sigma_1$	Major Principle Stress
$\sigma_3$	Minor Principle Stress